Environmental Science & Technology

Article

pubs.acs.org/est

Properties and Inflammatory Effects of Various Size Fractions of Ambient Particulate Matter from Beijing on A549 and J774A.1 Cells

Bin Wang,[†] Kexin Li,[‡] Wenjie Jin,[†] Yan Lu,[†] Yuzhong Zhang,[†] Guofeng Shen,[†] Rong Wang,[†] Huizhong Shen,[†] Wei Li,[†] Ye Huang,[†] Yanyan Zhang,[†] Xilong Wang,[†] Xiqing Li,[†] Wenxin Liu,[†] Hongying Cao,[‡] and Shu Tao[†,*]

[†]Laboratory for Earth Surface Processes, College of Urban and Environmental Sciences, Peking University, Beijing 100871, P.R. China

[‡]Institute of Geographic Sciences and Natural Resources Research, Chinese Academy of Sciences, Beijing 100101, P.R. China

ABSTRACT: Particulate matter (PM) is a major ambient air pollutant causing millions of premature deaths each year in China. The toxicity of PM is property and size dependent. In this study, ambient PM samples collected in Beijing were divided into five size fractions with nominal aerodynamic ranges of <0.40, 0.40−1.1, 1.1−3.3, 3.3−5.8, and 5.8−10 μm. Individual size fractions were characterized for a number of properties including particle size distribution, specific surface area, zeta potential, dithiothreitol (DTT)-based redox ability, and contents of water-soluble organic carbon (WSOC), polycyclic aromatic hydrocarbons (PAHs), selected metals, and endotoxin. Human adenocarcinomic alveolar epithelial cell line A549 and small mouse monocyte-macrophage cell line J774A.1 were tested for their relative viabilities and inflammatory effects (interleukine-8 for A549 and tumor necrosis factor-α for J774A.1) after exposure to PM of various sizes. It was found that PM specific area was positively correlated with WSOC, high molecular weight PAHs, DTT-based redox ability, negatively correlated with surface zeta potential and lithophile metals. Several trace metals from combustion sources were enriched in intermediate size fractions. For both endotoxin concentrations of the PM and PM induced inflammatory cytokine expressions by the two cell lines, there were general increasing trends as PM size increased with an exception of the finest fraction, which induced the highest inflammatory effects. It seems that the size dependence of cytokine expression was associated with a number of properties including endotoxin content, zeta potential, settling velocity, metal content, and DTT-based redox ability.

INTRODUCTION

Abundant evidence supports the idea that concentrations of ambient air-borne particulate matter (PM) are positively correlated with human mortality.[1,2] Extensive air pollution has been reported in China,[3] and millions of premature deaths can be attributed to inhalation exposure to PM each year.[4]

PM can be classified into size fractions and PM_{10} (<10 μm) is a typical example. PM_{10} can be further categorized into fine ($PM_{2.5}$, < 2.5 μm) and coarse (2.5 - 10 μm) fractions, while $PM_{0.1}$ (<0.1 μm) is referred as ultrafine particles.[5] Fine PM is derived mainly from the emissions of power plants, oil refineries, wildfires, household combustion, and other combustion sources, whereas ultrafine PM is either from various combustions directly or from secondary aerosol formation. On the other hand, coarse PM is commonly suspension derived from bare land and disturbed soil.[5] Therefore, the compositions of various PM size fractions may differ greatly. Fine PM often consists of sulfate, nitrate, ammonium, organic matter, crustal matter, rock dust, and elemental carbon, whereas surface dust, fly ash, crust element oxides, minerals, and biological fragments are major components of coarse PM.[6,7]

In vitro test using lung cell lines is a widely used fast-screening method for testing toxic effects of PM.[8] It is also useful for investigating toxicity machanism at the cell level.[9] Both human adenocarcinomic alveolar epithelial cell line A549 and small mouse monocyte-macrophage cell line J774A.1 are among the commonly used models. Of various adverse pulmonary effects, inflammation and oxidative stress damage induced by PM are two critical end points.[10,11] For example, Hetland et al. used A549 and primary rat type 2 cell lines to test the toxicity of ambient PM_{10} from a road tunnel.[10] Li et al. adopted murine macrophage cell line RAW 264.7 and human bronchial epithelial cell line BEAS-2B to investigate the cell toxicity mechanism of PMs from Los Angeles.[11] The results of many studies have revealed that PM toxicity is dependent on both size and composition. For example, it was found that secretion of proinflammatory molecules from A549 and J774A.1 cell lines could be induced by PM_{10} samples collected from various sites in Mexico City and the different toxicities among the samples could be attributed to the differences in sample size and composition.[12] However, there is no general agreement on how exactly the PM toxic effect was affected by size or composition. For example, relatively high cell toxicity of

Received: March 30, 2013
Revised: August 11, 2013
Accepted: August 19, 2013
Published: August 19, 2013

fine PM was observed and it was explained by the fact that PM in small size range allow better membrane penetration.[11,13,14] In some other studies, coarse PM were found to be more toxic than fine ones, likely due to high levels of endotoxin and transition metals and more intimate contact with cells.[10,15,16]

Physicochemical properties are also critical in terms of PM toxicity. A variety of properties including surface zeta potential, water-soluble organic carbon (WSOC), dithiothreitol (DTT)-ased redox ability, metals, endotoxin, and polycyclic aromatic hydrocarbons (PAHs) have been investigated for their influences on PM toxicity. It was reported that positive zeta potential allowed nanoparticles to damage the integrity of phagolysosomal membrane, leading to inflammation in lung cells.[17] In another study, it was revealed that Zn and Cu were more toxic to cells than Ni, Fe, Pb, or V.[18] Pulmonary and cardiovascular effects of PM have been demonstrated in in vivo studies.[19,20] It was found that PM collected in European cities could cause pulmonary inflammation and induce blood fibrinogen of spontaneously hypertensive rats. It was also found that the lactate dehydrogenase, proteins, and some inflammation parameters were correlated with metal and PAH contents.[19]

The objectives of this study were 2-fold: (1) to characterize properties of various size fractions of ambient atmospheric PM collected in Beijing, and (2) to investigate inflammatory effects of the PM, focusing on the differences among the size fractions. Both A549 and J774A.1 cell lines were used.

MATERIALS AND METHODS

Cell Models and Reagents. Both A549 and J774A.1 cell lines were purchased from Cell Resource Center, IBMS, China and were subcultured in our laboratory. RPMI Medium 1640 (RPMI) and Dulbecco's Modified Eagle Medium (DMEM) were used as culture medium for A549 and J774A.1, respectively. Both media contain 1% nonessential amino acids (NEAA), 100 U/mL penicillin, 100 mg/mL streptomycin sulfate, and 10% fetal bovine serum (FBS). RPMI, DMEM, NEAA, FBS, and trypsin-EDTA were from Gibco, USA. DTT, penicillin, and streptomycin sulfate were from Sigma-Aldrich, St. Louis, MO. Dichloromethane, *n*-hexane, methanol, silica gel (100−200 mesh) and granular anhydrous sodium sulfate were from Beijing Reagent, China. Silica gel was heated at 450 °C for 4 h, reactivated at 130 °C for 16 h. Anhydrous sodium sulfate was baked at 650 °C for 6 h. Phosphate buffered saline (PBS, pH 7.2−7.4) was prepared by mixing NaCl (8.5 g), Na_2HPO_4 (1.4 g), and NaH_2PO_4 (0.20 g) in 1.0 L ultrapure water.

PM Samples. PM of nine aerodynamic diameter ranges (<0.40, 0.40−0.70, 0.70−1.1, 1.1−2.1, 2.1−3.3, 3.3−4.7, 4.7−5.8, 5.8−9.0, and 9.0−10 μm) were collected on Peking University campus using a nine-stage cascade impactor (FA-3, Kangjie, China) at a flow rate of 28.3 L/min for 10 days from June 21th to 30th, 2010. Glass fiber filters were used for the first stage (<0.40 μm), whereas aluminum foils were used for all other stages. The nine fractions were pooled into five with nominal diameter ranges of <0.4 (F1), 0.40−1.1 (F2), 1.1−3.3 (F3), 3.3−5.8 (F4), and 5.8−10 μm (F5), respectively. The particles were removed from the filters or foil with 30 mL methanol ultrasonically for 5 min. The suspensions were concentrated to 1 mL using rotary evaporator at 37 °C and freeze-dried (EYELA-FDU-830, Tokyo Rikakikai, Japan). The PM were resuspended to 5 mg/mL in methanol as stock solutions. A control (without filter or PM) and a procedure blank for F1 (with glass fiber filter but without PM) were prepared using the exactly same procedure. It should be pointed out that partial loss of volatile chemicals during the extraction and concentration could not be avoided. Some particles, especially fine particles could not be totally recovered from the filter by the extraction. Therefore, the results should be interpolated with care.

PM Characterization. Size distribution and zeta potential of the PM fractions were measured using a Zetasizer Nano (ZS90, Malvern, UK) and the samples were diluted to 0.1 mg/mL using cell culture medium containing 10% fetal bovine serum, ultrasonicated for 1 min, and well mixed by votex for about 5 s before the measurement. For WSOC measurement, PM suspension (0.1 mg/mL) was soaked for 16 h under shaking (100 rpm) at 25 °C and filtered through quartz filters (0.2 μm).[21] The filtrate was measured for WSOC using a total carbon analyzer (Shimadzu 5000A, Japan). Fifteen U.S. Environmental Protection Agency priority PAHs including acenaphthylene (ACY), acenaphthene (ACE), fluorene (FLU), phenanthrene (PHE), anthracene (ANT), fluoranthene (FLA), pyrene(PYR), benz[a]anthracene (BaA), chrysene (CHR), benzo[b]fluoranthene (BbF), benzo[k]fluoranthene (BkF), benzo[a]pyrene (BaP), dibenz[a,h]anthracene (DahA), benzo-[g,h,i]perylene (BghiP), and indeno[1,2,3-cd]pyrene (IcdP) were extracted using a microwave accelerated reaction system (CEM, Weddington, NC) and measured using a gas chromatograph−mass spectrometer (GC/MS, Agilent 6890/5973) following an extraction−cleanup−analysis precedure described previsouly.[22] For metal analysis, PM samples were digested using a mixture of HNO_3 and $HClO_4$ following a procedure described in the literature.[23] The metal concentrations were determined using an inductively coupled plasma−atomic emission spectrometry (Optima 3300DV, Perkin-Elmer, Waltham, MA).[23] For DTT assay, the PM sample was incubated in Tris buffer with 10 μM DTT at pH 8.9 for 20 min. After spiking with 0.4 mL of 10% trichloroacetic acid, it was mixed with 0.4 mL of 0.4 M Tris-HCl and measured using a microplate reader (Multiskan Mk3, Thermo Electron, Finland).[24] Endotoxin was measured using Limulus amebocyte lysate assay kits (Chinese Horseshoe Crab Reagent, China) and the microplate reader, following the procedure provided by the kit manufacturer.

PM Exposure and Cell Cultivation. The five PM fractions, a control (without PM) and a procedure blank for F1 (with glass fiber filter but without PM) were cultivated. The PM samples were diluted to 50 μg/mL using either RPMI (for A549 cells) or DMEM (for J774A.1 cells) without FBS for the cultivation, and fully dispersed by sonication (60 s) and vortex (30 s). To each used well on 96-well plates, approximately 50 000 cells were precultured. The PM suspensions (including the control and blank) were added to individual wells (100 μL each). The outer peripheral wells of the plates were not used for sample cultivation and filled with sterile PBS to reduce the evaporation from the exposure cells. Eighteen wells were used as duplicates for each treatment to reduce variation among individual wells. The plates were incubated at 37 °C in a CO_2-incubator (5% CO_2, Sanyo, Japan) for 24 or 48 h. To each well, 10 μL FBS was added after the first 6 h. To each of the 48 h incubation wells, 40 μL culture medium was added to each well after 24 h to compensate evaporation loss. For each treatment, the samples from 18 cultured wells as duplicates were randomly pooled into three composite samples (6 each) for cytokines measuring.

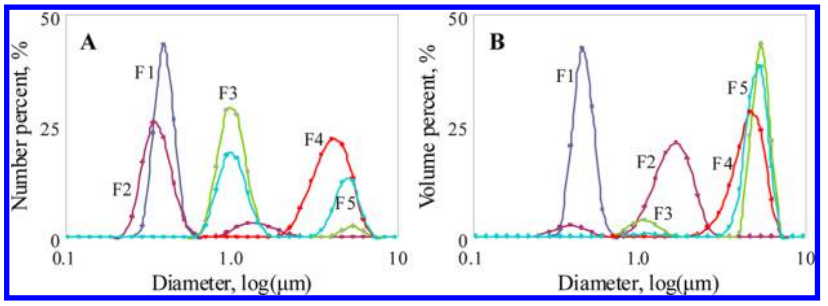

Figure 1. Size distributions of the five PM fractions. (A) number distribution (B) volume distribution.

Table 1. PAH Concentrations in the Five PM Size Fractions As Means and Standard Deviations[a]

		concentration, ng/mg						significant groups				
PAHs	MW[b]	F1	F2	F3	F4	F5	*p*	F1	F2	F3	F4	F5
ACY	152	1.4 ± 0.86	1.1 ± 0.26	1.2 ± 0.39	1.5 ± 0.16	1.0 ± 0.92	0.904	*a*	*a*	*a*	*a*	*a*
ACE	154	7.9 ± 3.9	6.2 ± 1.3	7.6 ± 1.9	9.0 ± 0.79	5.8 ± 0.76	0.763	*a*	*a*	*a*	*a*	*a*
FLU	166	1.4 ± 0.86	1.1 ± 0.26	1.2 ± 0.39	1.5 ± 0.16	1.0 ± 0.92	0.906	*a*	*a*	*a*	*a*	*a*
PHE	178	7.9 ± 3.9	6.2 ± 1.3	7.6 ± 1.9	9.0 ± 0.79	5.8 ± 0.76	0.913	*a*	*a*	*a*	*a*	*a*
ANT	178	47 ± 45	33 ± 5.5	36 ± 4.0	51 ± 1.2	44 ± 14	0.771	*a*	*a*	*a*	*a*	*a*
FLA	202	250 ± 22	200 ± 16	220 ± 39	290 ± 19	250 ± 17	0.928	*a*	*a*	*a*	*a*	*a*
PYR	202	49 ± 67	50 ± 6.0	54 ± 4.9	84 ± 8.2	58 ± 0.10	0.902	*a*	*a*	*a*	*a*	*a*
BaA	228	170 ± 15	180 ± 0.50	160 ± 9.3	210 ± 34	200 ± 8.1	0.028	*b*	*b*	*a*	*a*	*a*
CHR	228	150 ± 14	160 ± 7.5	150 ± 7.0	200 ± 3.1	170 ± 13	0.001	*c*	*c*	*b*	*a*	*a*
BbF	252	8.7 ± 1.8	7.9 ± 2.0	4.8 ± 0.049	3.1 ± 0.95	4.3 ± 0.77	0.000	*c*	*d*	*b*	*a*	*a*
BkF	252	21 ± 1.3	21 ± 1.5	16 ± 1.1	8.6 ± 0.28	10 ± 1.9	0.000	*c*	*c*	*b*	*a*	*a*
BaP	252	24 ± 0.37	28 ± 4.6	15 ± 1.2	5.2 ± 0.071	5.2 ± 1.1	0.001	*c*	*c*	*b*	*a*	*a*
IcdP	276	19 ± 1.6	23 ± 2.5	14 ± 0.099	4.7 ± 0.16	3.8 ± 0.36	0.000	*c*	*d*	*b*	*a*	*a*

[a]The differences among the fractions were tested using analysis of variance and multiple comparison for individual PAHs. The results are presented as *p* values and significant groups (groups with significant difference in between) marked as "*a*", "*b*", "*c*", and "*d*". [b]MW: molecular weight.

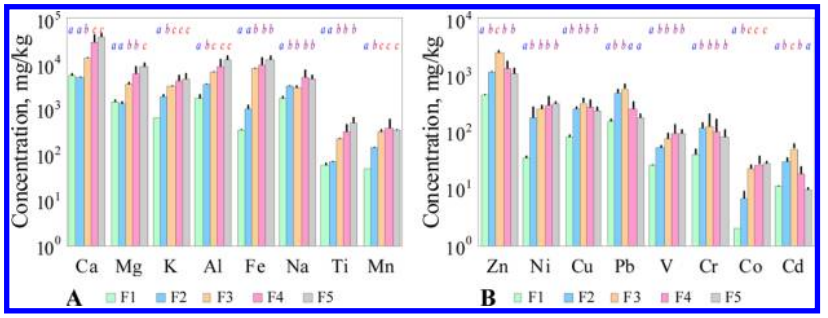

Figure 2. Concentrations of 16 metals in the five size fractions. (A) major elements, (B) trace elements. The results are presented as means and standard deviations of two duplicate measurements, The statistical differences ($\alpha = 0.05$) among the fractions of individual metals were tested using multiple comparison. Based on the results, the five fractions of each metal can be classified into insignificant groups of "*a*", "*b*", or "*c*". There were significant differences among the fractions in different groups but no significant difference among the fractions within the same group.

Table 2. PM Properties Including Diameter, Specific Surface Area, WSOC, DTT-Based Redox Activity, And Endotoxin Concentration of the Five Size Fractions

PM property	F1	F2	F3	F4	F5
average diameter/μm	0.40 ± 0.030	0.54 ± 0.25	1.3 ± 0.62	4.1 ± 0.57	2.6 ± 1.2
specific surface area/μm^{-1}	15 ± 1.1	15 ± 3.1	5.7 ± 0.89	1.6 ± 0.24	4.1 ± 1.4
WSOC/(mgC/mg)	0.12 ± 0.016	0.15 ± 0.012	0.086 ± 0.0092	0.068 ± 0.00069	0.069 ± 0.0054
DTT/(nmol/(min·μg))	0.021 ± 0.00042	0.016 ± 0.00075	0.011 ± 0.00055	0.0080 ± 0.00093	0.0081 ± 0.0010
endotoxin/(EU/mg)	9.4 ± 0.57	3.0 ± 0.081	7.6 ± 0.099	10 ± 0.16	17 ± 0.92

MTT (3-(4,5-Dimethylthiazol-2-yl)-2,5-diphenyltetrazolium Bromide) Assay. A mixture of 20 μL MTT (5 mg/mL in sterilized PBS solution) and 200 μL culture medium was added to each well after the exposure. The plates were incubated again at 37 °C and 5% CO_2 for 4 h and centrifuged (1000*g*, 10 min). After the supernatant was removed from the well, 200 μL PBS was added. The supernatant was removed again after recentrifugation. After addition of 200 mL DMSO to each well, formazan crystal desolved in DMSO was measured at 490 nm using the microplate reader.

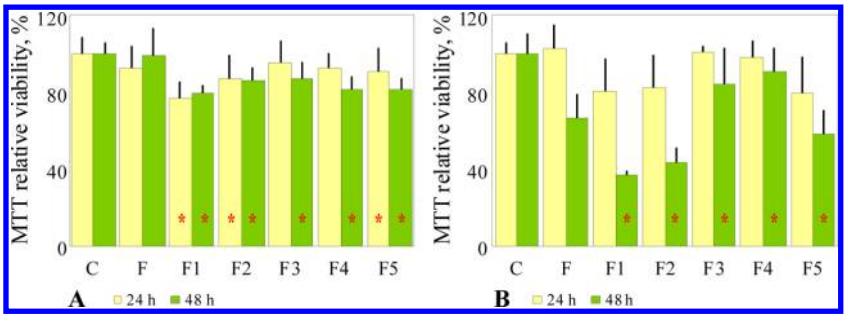

Figure 3. MTT relative viabilities of A549 (A) and J774A.1 (B) cell lines after 24 or 48 h incubation with the five PM fractions, a control (C, without PM), and a procedure blank for F1 (F, with fiber but without PM). The results are presented as means and standard deviations of 12 duplicate measurements. A multiple comparison was conducted to test the significance (α = 0.05) between the samples and the controls and among the five fractions. The tests were performed for A549 and J774A.1 cell lines and for 24 and 48 h, individually. The samples with significantly different from the control are marked with "*". For the tests among samples, there were two significant groups (F1) and (F2, F3, F4, and F5) for A549 cell line at 24 h, and no significant difference among the five fractions for A549 at 48 h. For J774A.1 cell line, there were two significant groups (F1, F2, F5) and (F2, F4) at 48 h, but no significant difference at 24 h.

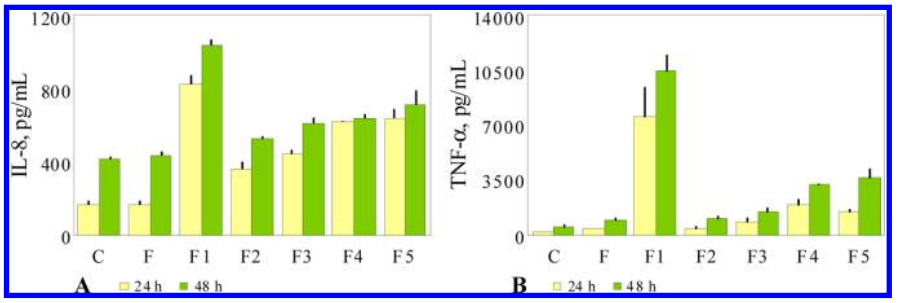

Figure 4. IL-8 expressions of A549 cell line (A) and TNF-a expressions of J774A.1 cell line (B) induced by 24 or 48 h exposure to the five size fractions, a control (C, without PM), and a procedure blank for F1 (F, with fiber but without PM). The results are presented as means and standard deviations. A multiple comparison was conducted to test the significance (α = 0.05) between the samples and the controls and among the five fractions. The tests were performed for A549 and J774A.1 cell lines and for 24 and 48 h, individually. For A549, the three significant groups were (F1), (F2, F3), and (F4, F5) for 24 h and (F1), (F2), and (F3, F4, F5) for 48 h. For J774A.1, the three significant groups were (F1, F2), (F3), and (F4, F5) for both 24 and 48 h experiments.

Cytokines. Human interleukine-8 (IL-8) and small mouse tumor necrosis factor-α (TNF-α) in the centrifuged (1000*g* for 10 min) supernates were detected using enzyme-linked immunoabsorbant assay using the microplate reader at 450 nm according to the manufacturer's guidelines (Wuhan Boster, China).

Data Analysis. The measurements were conducted in either duplicate (cytokines, PAHs, WSOC, and metals), triplicate (zeta potential, size distribution, and endotoxin), or hexaplicate (MTT assay). The results are presented as means and standard deviations. Statistical analysis was performed using SPSS (v. 13.0) at significant level of 0.05.

RESULTS AND DISCUSSION

Size Distribution and Surface Zeta Potential. Size distributions of the PM fractions are shown in Figure 1 as either number (A) or volume (B). Significant difference among the fractions is demonstrated. The mean diameters (number) were 0.40 ± 0.03, 0.54 ± 0.25, 1.3 ± 0.62, 4.1 ± 0.57, and 2.6 ± 1.2 μm for F1 through F5. Unexpectedly, the mean diameter of F5 was smaller than that of F4, likely due to the bimodal size distribution of F5 with an extra peak around 1.0 μm, likely originated from breakdown of particles during ultrasonication.[25] Similar bimodal distributions were observed for F2 and F4. The measured size distribution using Zetasizer Nano was hydrodynamic, instead of aerodynamic range. Therefore, the size (also the specific surface area) measurements are only meaningful in relative terms and are not directly compatible to those in the literature. Only the trends of size effects on PM properties and toxicities are discussed. The mean specific surface areas measured were 15 ± 1.1, 15 ± 3.1, 5.7 ± 0.89, 1.6 ± 0.24, and 4.1 ± 1.4 μm^{-1} for F1 through F5, which were not exactly in the same order of the mean size, because of the bimodal distributions. It is believed that stability of the suspension can be well maintained during the experiment by FBS (10% v/v), which is an effective dispersing agent.[26]

The measured zeta potentials were all negative (−28 ± 0.81, −23 ± 0.50, −15 ± 0.21, −12 ± 0.23, and −12 ± 0.18 mV for F1 through F5), which are similar to those reported in the literature.[27] The negative charge of the PM collected in Beijing is believed to be caused by proton dissociation[7] and sorption of negatively charged proteins from the media.[28] With relatively high organic carbon contents and larger specific surface areas, fine PM can adsorb more than coarse ones, leading to significantly positive correlation between zeta potential and size (r = 0.73, p < 0.05) and negative correlation between zeta potential and specific area (r = −0.95, p < 0.05).

WSOC, PAHs, and Metals. The measured WSOC concentrations were 0.12 ± 0.016, 0.15 ± 0.012, 0.086 ± 0.0092, 0.068 ± 0.00069, and 0.069 ± 0.0054 mgC/mg for F1 through F5, which were correlated with PM size negatively (r = −0.67, p < 0.05) and specific area positively (r = 0.88, p < 0.05). Although mean diameter of F1 was smaller than that of F2, WSOC of F2 was higher than that of F1 (p < 0.05), likely due to the fact that there was a fraction of the finest PM in the

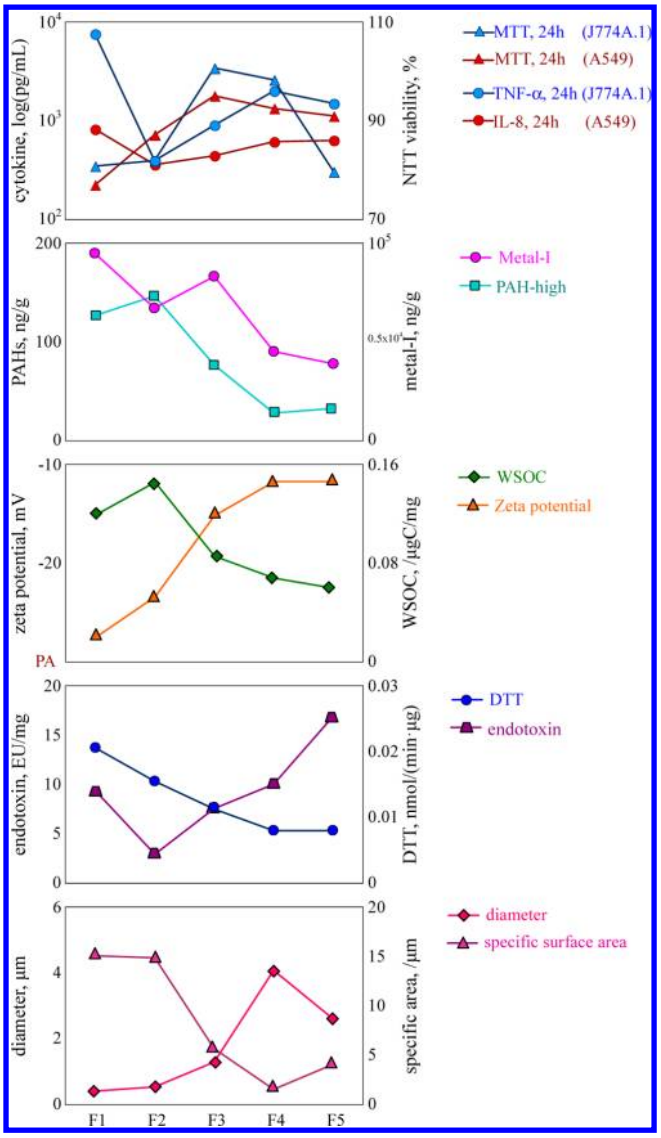

Figure 5. Trends of the measured properties and toxicities of the five PM size fractions from F1 to F5, showing inter-relationship among them. "PAH-high" stands for the PAHs with high molecular weight (from BaA to IcdP); "Metal-I" includes K, Na, Ca, Mg, Al, Fe, Mn, Ti, Ni, Co, and V.

bimodal F2. In fact, specific areas of F1 and F2 were very close to each other and specific area of F4 was even smaller than that of F5. Similar dependence of WSOC on PM size has been reported for samples collected from Helsinki,[29] Tai Mountain,[30] and Zurich.[31] It was believed that WSOC contents of PM are strongly affected by their sources and chemical composition.[5] WSOC in fine particles tend to be higher than that in coarse particles,[6] because semivolatile organic carbon, acids, and other carbons derived from high temperature combustion are major compositions of fine and ultrafine particles, while suspensions are major compositions of coarse PM.

Among the 15 PAHs, the concentrations of DahA and BghiP were lower than the detection limits and are not included in the discussion. The total concentrations of the remained 13 PAHs were 8.6×10^2, 8.5×10^2, 7.4×10^2, 9.0×10^2, and 7.7×10^2 ng/mg for F1 through F5. Detailed data are shown in Table 1. The concentrations of individual PAHs are compared among the five fractions using analysis of variance and multiple comparisons (LSD) and the results are also included in Table 1. The differences among the five fractions were not significant ($p > 0.05$) for low molecular weight PAHs from ACY to PYR (PAH-low, 152 - 202), but significant ($p < 0.05$) for high molecular weight ones from BaA to IcdP (PAH-high, 228–276). Significant correlation between the total concentration of 6 PAH-high and PM size ($r = -0.91$, $p < 0.05$) or specific area ($r = 0.97$, $p < 0.05$) can be seen. It has also been reported previously that PAHs with median to high molecular weight (202–278) in ambient aerosol samples collected from Tianjin were mainly associated with fine particles of less than 2.1 μm, whereas PAHs with molecular weight between 128 and 178 were more or less evenly distributed among fine and coarse fractions.[32] It should be noted that loss of volatile low molecular weight compounds during sample handling could not be totally avoided.

The measured metal concentrations are shown in Figure 2. Significant difference among the five size fractions can be seen for all metals ($p < 0.05$). The metals can be generally classified into two categories with distinguished size distribution patterns. The concentrations of K, Na, Ca, Mg, Al, Fe, Mn, Ti, Ni, Co, and V increased as the particle sized increased. For Cu, Cd, Pb, Zn, and Cr, the highest concentrations occurred in the fraction with size between 1.1 and 3.3 μm. The metals in the first category are mainly rock-forming elements associated with coarse particles,[33] which are largely suspensions. The trace metals in the second category are mainly from combustion sources.[6,34] Among other studies on metal size distribution in atmospheric aerosols from various sites, Samara et al. found that the highest abundances of Cu, Cd, Pb, Cr, Ni, and Mn in aerosols collected in Athens occurred in particles between 1.3 and 2.7 μm, whereas Fe and V had highest contents in particles from 2.7 to 6.7 μm.[35] It should be noted that the sizes reported in this study were measured after the particles were removed from the filters and are different from the nominal aerodynamic size reported in the literature.

Endotoxin and DTT-Based Redox Ability. Endotoxin in the samples were 9.4 ± 0.57 (F1), 3.0 ± 0.081 (F2), 7.6 ± 0.099 (F3), 10 ± 0.16 (F4), and 17 ± 0.92 (F5) EU/mg, which were much lower than those (30.1–49.3 EU/mg) reported for PM_{10} collected from Mexico City.[16] It is not surprising to see that endotoxin generally increased as particle size increased since it is believed that endotoxin originate from dead gram-negative bacteria, which tend to be associated with coarse particles.[15] The only exception, F1, with endotoxin higher than those in F2 and F3 can not be well explained at this stage, but similar enrichment of endotoxin in ultrafine particles has also been documented previously.[36,37] Of all the properties tested, endotoxin was the only one with no significant correlation with PM size or specific area.

For the five size fractions, the measured DTT were 0.021 ± 0.00042 (F1), 0.016 ± 0.00075 (F2), 0.011 ± 0.00055 (F3), 0.0080 ± 0.00093 (F4), and 0.0081 ± 0.0010 (F5) nmol/(min·μg). Similar to PAHs and WSOC, DTT decreased from F1 to F5, with the exception that no significant difference was observed between F4 and F5. DTT was also correlated with PM size negatively ($r = -0.72$, $p < 0.05$), and specific area positively ($r = 0.87$, $p < 0.05$). Similar trends have been reported in the literature.[11,24] Such correlations are expected since water-soluble compounds especially reactive quinones are believed to be responsible for reactive oxygen species (ROS) formed during DTT assay,[38] while these chemicals are primarily

associated with fine and ultrafine particles in ambient air.[39] The means and standard deviations of chemical and physical properties are listed in Table 2.

Cell Viability. Figure 3 shows MTT relative viabilities for both A549 and J774A.1 cells after 24 or 48 h exposure to the five PM fractions. Effect of the fibers ("F" in Figure 3) was only observed for J774A.1 after 48 h cultivation. As discussed above, most properties measured in this study were either negatively (zeta potentials and lithophile metals) or positively (WSOC, PAH-high, and DTT-based redox activity) correlated with specific surface area (size). Although MTT values in several size fractions at 48 h were significantly different from those in other fractions and those at 24 h, there is not general trend of size dependence for cell viability.

Relative viabilities of A549 exposed to the five PM fractions were all above 80%, even though many of them are significantly lower than that of the control ($p < 0.05$). For F4 and F5, MTT of 48 h were slightly lower than those of 24 h ($p < 0.05$), while no such difference was found for the other three fractions. The slight inhibition of the PM exposure on A549 cell viability was generally lower than those reported in the literature[10,40] and would not have a significant effect on cytokine measurements. J774.A1 cells appear to be more sensitive than A549 in terms of MTT viability under the PM exposure. Although no significant effect ($p > 0.05$) on J774.A1 cells was observed after 24 h exposure to all five size fractions, likely due to relatively high variation, significant inhibition was found for some fractions, especially the finest fractions of F1 and F2 at 48 h. The results of a study on atmospheric particles from Mexico City revealed that the J774.A1 cells could be inhibited and the toxicity difference between fine and coarse PM depended on sampling locations.[16] Still, most values of relative viability of J774.A1 cells determined in this study were above 60% and were higher than those reported in the literature for inflammatory comparison studies at similar conditions.[10,40]

Cytokines. Cytokines measured in this study included IL-8 for A549 cells and TNF-α for J774A.1 cells and the results are shown in Figure 4. No significant difference between the control (C) and fiber blank (F) was found for all cases (IL-8 and TNF-α at 24 and 48 h) ($p > 0.05$), suggesting that glass fibers in F1, which could not be totally removed, did not cause any significant effect on the release of the cytokines.

For both cell lines, cytokines released after the exposure were significantly higher than those in the control ($p < 0.05$), indicating strong inflammatory effects. In addition, the measured IL-8 and TNF-α after 48 were significantly higher than those after 24 h for most size fractions ($p < 0.05$), with only exceptions of IL-8 in F4 and F5. It appears that the cytokines were continuously generated during the entire experimental period of 48 h.

There were studies focusing on the dependence of PM toxicity on size distribution using in vitro assay,[10,16] in vivo experiment,[14] or epidemiological survey.[13,41] The outcomes of these studies varied in terms of direction of the size effect. For example, Osornio-Vargas et al. found that secretions of TNF-α and IL-6 from J774A.1 cells induced by PM_{10} were higher than those induced by $PM_{2.5}$.[16] Hetland et al. reported that coarse PM could induce more inflammatory cytokine expressions in both A549 and primary rat type 2 cells.[10] However, other researchers found that fine PM with higher organic components and DTT-based redox activity could induce higher ROS expression, causing higher cell toxicity (Li et al., 2003).[11] It is worth to note that the PM samples tested in these studies were from different sources. The samples used in the above-mentioned case studies were from urban ambient environment (Mexico City), a road tunnel (Trondheim, Norway), or both urban and background sites (Los Angeles), respectively, and they are not directly comparable. It appears that size dependence of the inflammatory effects of PM may rely on their points of origin and their compositions.

In this study using five size fractions, the dependence of inflammatory expressions on PM size was not monotonic. Among the five fractions, the highest inflammatory cytokine expressions in both A549 and J774A.1 cells were induced by the finest fraction (F1), whereas the inflammatory effects increased as the particle size increased from F2 to F5. Among all particle properties measured in this study, none of them had exactly the same trends as cytokines. However, the trend of the measured endotoxin (increased with size except F1) was similar to that of cytokines, even though it could not help to explain the fact that the highest concentrations occurred in the finest (F1) rather than the coarsest (F5) fraction. It was reported in the literature that recombinant endotoxin-neutralizing protein (inhibitor of endotoxin) can reduce cytokine secretion induced by PM_{10} collected from southeast area of Mexico City, suggesting that PM_{10} can induce cytotoxicity in vitro through an endotoxin-dependent mechanism.[16] On the other hand, toxic effects of $PM_{2.5}$ are likely caused by a transition metal-dependent mechanism.[16] In the future study, it will be interesting to look into the mechanism causing the inflammatory expression. For example, one hypothesis can be tested is that the ultrafine particles may get inside of cells causing inflammatory responses. In addition, antibodies against toll-like receptor (TLR) can be used to test possible TLR pathways.

The negative correlation between zeta potential and cytokines ($p < 0.05$) may also help to explain the general trend that inflammatory effects increased as particle size increased (with the exception of F1). Since cell surface is negatively charged, the extent of interaction between PM and cell surface is affected by PM surface zeta potential.[42] It was reported that negatively charged particles can hardly be adsorbed on the cell surface.[43] Moreover, large particles are likely to have more opportunity of contacting cells simply due to higher gravity. In one of our preliminary experiments, significant difference in settling rates were found among the five size fractions and it took much longer time for fine PM to settle. In fact, differences in gravitational settling of particles with different size ranges is an intrinsic limitation of the in vitro cell model.[44] The positive correlation between the measured cytokines and particle size from F2 to F5 may also be associated with some metals. It is possible that the difference in concentrations of a group of lithophile metals among various PM size fractions (Figure 2) could cause differences in the inflammatory effects. Cell toxicity caused by a number of transition metals has been reported in the literature.[19] Hetland et al. have found that coarse PM with higher metal contents could induce more inflammatory cytokine expressions in human A549 cells and primary rat type 2 cell than fine PM with lower metal contents.[10] It was also noted that DTT-based redox activity maximized in F1 fraction in this study, which could be an important factor affecting the generation of cytokines in the finest fraction. The relationship between ROS generation in cells and their inflammatory cytokine expression has been reported previously.[45]

In sum, it seems likely that more than one factor, very likely including some others not measured in this study, contributed effectively to the inflammatory cytokine expression. The apparent trend of the inflammatory effects probably involves synergistic effects. These complicated relationships are summarized in Figure 5. It should be noted that the correlation can not be simply applied to other samples due to complexity of PM. More carefully designed studies are needed for a better understanding of major factors affecting their toxicity.

AUTHOR INFORMATION

Corresponding Author

*Phone: 86-10-62751938; e-mail: taos@pku.edu.cn.

Notes

The authors declare no competing financial interest.

ACKNOWLEDGMENTS

This work was supported by the National Science Foundation of China (Grant No.41130754, 41101490, and 41001343). We thank Dr. Yu Yang of Yale University for his valuable comments, Dr. Xiangdong Li of Hong Kong Polytechnic University for metal analysis, and Dr. Jianying Hu of Peking University for supporting cytokine measurement. R.M. Coveney of the University of Missouri-Kansas City commented on a draft of the manuscript.

REFERENCES

(1) Pope, C. A.; Dockery, D. W. Health effects of fine particulate air pollution: Lines that connect. *J. Air Waste Manage* **2006**, *56*, 709−742.

(2) Xu, Z. Y.; Yu, D. G.; Jing, L. B.; Xu, X. P. Air pollution and daily mortality in Shenyang, China. *Arch. Environ. Health* **2000**, *55*, 115−120.

(3) Kan, H.; Chen, R.; Tong, S. Ambient air pollution, climate change, and population health in China. *Environ. Int.* **2012**, *42*, 10−19.

(4) Zhang, J. F.; Smith, K. R. Household Air pollution from coal and biomass fuels in China: Measurements, health impacts, and interventions. *Environ. Health Perspect.* **2007**, *115*, 848−855.

(5) Araujo, J. A.; Nel, A. E. Particulate matter and atherosclerosis: Role of particle size, composition and oxidative stress. *Part. Fibre Toxicol.* **2009**, *6*. DOI: 10.1186/1743-8977-6-24.

(6) Wilson, W. E.; Suh, H. H. Fine particles and coarse particles: Concentration relationships relevant to epidemiologic studies. *J. Air Waste Manage.* **1997**, *47*, 1238−1249.

(7) Hu, M., He, L. Y. Huang, X. F. *Physical-Chemical Characteristics, Sources and Formation Mechanisms of Airborne Fine Particles and Ultrafine Particles in Beijing* (In Chinese); Science Press: Beijing, 2009, p 282.

(8) Ayres, J. G.; Borm, P.; Cassee, F. R.; Castranova, V.; Donaldson, K.; Ghio, A.; Harrison, R. M.; Hider, R.; Kelly, F.; Kooter, I. M.; Marano, F.; Maynard, R. L.; Mudway, I.; Nel, A.; Sioutas, C.; Smith, S.; Baeza-Squiban, A.; Cho, A.; Duggan, S.; Froines, J. Evaluating the toxicity of airborne particulate matter and nanoparticles by measuring oxidative stress potential - A workshop report and consensus statement. *Inhal. Toxicol.* **2008**, *20*, 75−99.

(9) Donaldson, K.; Borm, P., *Particle Toxicology*, 1st ed.; CRC: Boca Raton, FL, 2006.

(10) Hetland, R. B.; Cassee, F. R.; Refsnes, M.; Schwarze, P. E.; Lag, M.; Boere, A. J. F.; Dybing, E. Release of inflammatory cytokines, cell toxicity and apoptosis in epithelial lung cells after exposure to ambient air particles of different size fractions. *Toxicol. In Vitro* **2004**, *18*, 203−212.

(11) Li, N.; Sioutas, C.; Cho, A.; Schmitz, D.; Misra, C.; Sempf, J.; Wang, M. Y.; Oberley, T.; Froines, J.; Nel, A. Ultrafine particulate pollutants induce oxidative stress and mitochondrial damage. *Environ. Health. Perspect* **2003**, *111*, 455−460.

(12) Alfaro-Moreno, E.; Martinez, L.; Garcia-Cuellar, C.; Bonner, J. C.; Murray, J. C.; Rosas, I.; Rosales, S. P. D.; Osornio-Vargas, A. R. Biologic effects induced in vitro by PM_{10} from three different zones of Mexico City. *Environ. Health. Perspect* **2002**, *110*, 715−720.

(13) Schwartz, J. Particulate air-pollution and daily mortality in Detroit. *Environ. Res.* **1991**, *56*, 204−213.

(14) Wegesser, T. C.; Franzi, L. M.; Mitloehner, F. M.; Eiguren-Fernandez, A.; Last, J. A. Lung antioxidant and cytokine responses to coarse and fine particulate matter from the great California wildfires of 2008. *Inhal. Toxicol.* **2010**, *22*, 561−570.

(15) Monn, C.; Becker, S. Cytotoxicity and induction of proinflammatory cytokines from human monocytes exposed to fine ($PM_{2.5}$) and coarse particles ($PM_{10-2.5}$) in outdoor and indoor air. *Toxicol. Appl. Pharmacol.* **1999**, *155*, 245−252.

(16) Osornio-Vargas, A. R.; Bonner, J. C.; Alfaro-Moreno, E.; Martinez, L.; Garcia-Cuellar, C.; Rosales, S. P. D.; Miranda, J.; Rosas, I. Proinflammatory and cytotoxic effects of Mexico city air pollution particulate matter in vitro are dependent on particle size and composition. *Environ. Health Perspect* **2003**, *111*, 1289−1293.

(17) Cho, W. S.; Duffin, R.; Thielbeer, F.; Bradley, M.; Megson, I. L.; MacNee, W.; Poland, C. A.; Tran, C. L.; Donaldson, K. Zeta potential and solubility to toxic ions as mechanisms of lung inflammation caused by metal/metal oxide nanoparticles. *Toxicol. Sci.* **2012**, *126*, 469−477.

(18) Prieditis, H.; Adamson, I. Y. R. Comparative pulmonary toxicity of various soluble metals found in urban particulate dusts. *Exp. Lung Res.* **2002**, *28*, 563−576.

(19) Gerlofs-Nijland, M. E.; Rummelhard, M.; Boere, A. J. F.; Leseman, D. L. A. C.; Duffin, R.; Schins, R. P. F.; Borm, P. J. A.; Sillanpaa, M.; Salonen, R. O.; Cassee, F. R. Particle induced toxicity in relation to transition metal and polycyclic aromatic hydrocarbon contents. *Environ. Sci. Technol.* **2009**, *43*, 4729−4736.

(20) Gerlofs-Nijland, M. E.; Totlandsdal, A. I.; Kilinç, E.; Boere, A. J.; Fokkens, P. H.; Leseman, D. L.; Sioutas, C.; Schwarze, P. E.; Spronk, H. M.; Hadoke, P. W.; Miller, M. R.; Cassee, F. R. Pulmonary and cardiovascular effects of traffic-related particulate matter: 4-week exposure of rats to roadside and diesel engine exhaust particles. *Inhal. Toxicol.* **2010**, *22*, 1162−1173.

(21) Favez, O.; Sciare, J.; Cachier, H.; Alfaro, S. C.; Abdelwahab, M. M. Significant formation of water-insoluble secondary organic aerosols in semi-arid urban environment. *Geophys. Res. Lett.* **2008**, *35*.

(22) Wang, B.; Xue, M.; Lv, Y.; Yang, Y.; Zhong, J. J.; Su, Y. H.; Wang, R.; Shen, G. F.; Wang, X. L.; Tao, S. Cell absorption induced desorption of hydrophobic organic contaminants from digested soil residue. *Chemosphere* **2011**, *83*, 1461−1466.

(23) Lee, C. S. L.; Li, X. D.; Zhang, G.; Li, J.; Ding, A. J. Heavy metals and Pb isotopic composition of aerosols in urban and suburban areas of Hong Kong and Guangzhou, South China—Evidence of the long-range transport of air contaminants. *Atmos. Environ.* **2007**, *41*, 432−447.

(24) Cho, A. K.; Sioutas, C.; Miguel, A. H.; Kumagai, Y.; Schmitz, D. A.; Singh, M.; Eiguren-Fernandez, A.; Froines, J. R. Redox activity of airborne particulate matter at different sites in the Los Angeles Basin. *Environ. Res.* **2005**, *99*, 40−47.

(25) Kim, S.; Jaques, P. A.; Chang, M. C.; Froines, J. R.; Sioutas, C. Versatile aerosol concentration enrichment system (VACES) for simultaneous in vivo and in vitro evaluation of toxic effects of ultrafine, fine and coarse ambient particles—Part I: Development and laboratory characterization. *J. Aerosol Sci.* **2001**, *32*, 1281−1297.

(26) Ji, Z. X.; Jin, X.; George, S.; Xia, T. A.; Meng, H. A.; Wang, X.; Suarez, E.; Zhang, H. Y.; Hoek, E. M. V.; Godwin, H.; Nel, A. E.; Zink, J. I. Dispersion and stability optimization of TiO_2 nanoparticles in cell culture media. *Environ. Sci. Technol.* **2010**, *44*, 7309−7314.

(27) Veronesi, B.; de Haar, C.; Lee, L.; Oortgiesen, M. The surface charge of visible particulate matter predicts biological activation in human bronchial epithelial cells. *Toxicol. Appl .Pharm.* **2002**, *178*, 144−154.

(28) Limbach, L. K.; Wick, P.; Manser, P.; Grass, R. N.; Bruinink, A.; Stark, W. J. Exposure of engineered nanoparticles to human lung

epithelial cells: Influence of chemical composition and catalytic activity on oxidative stress. *Environ. Sci. Technol.* **2007**, *41*, 4158−4163.
(29) Timonen, H.; Saarikoski, S.; Tolonen-Kivimaki, O.; Aurela, M.; Saarnio, K.; Petaja, T.; Aalto, P. P.; Kulmala, M.; Pakkanen, T.; Hillamo, R. Size distributions, sources and source areas of water-soluble organic carbon in urban background air. *Atmos. Chem. Phys.* **2008**, *8*, 5635−5647.
(30) Wang, G. H.; Kawamura, K.; Umemoto, N.; Xie, M. J.; Hu, S. Y.; Wang, Z. F. Water-soluble organic compounds in $PM_{2.5}$ and size-segregated aerosols over Mount Tai in North China Plain. *J. Geophys. Res., [Atmos.]* **2009**, *114*, D19208.
(31) Minguillon, M. C.; Querol, X.; Baltensperger, U.; Prevot, A. S. H. Fine and coarse PM composition and sources in rural and urban sites in Switzerland: Local or regional pollution? *Sci. Total Environ.* **2012**, *427*, 191−202.
(32) Wu, S. P.; Tao, S.; Liu, W. X. Particle size distributions of polycyclic aromatic hydrocarbons in rural and urban atmosphere of Tianjin, China. *Chemosphere* **2006**, *62*, 357−367.
(33) Clayton, R. N.; Hinton, R. W.; Davis, A. M. Isotopic variations in the rock-forming elements in meteorites. *Philos. Trans. R. Soc., A* **1988**, *325*, 483−501.
(34) Wang, X. L.; Sato, T.; Xing, B. S. Size distribution and anthropogenic sources apportionment of airborne trace metals in Kanazawa, Japan. *Chemosphere* **2006**, *65*, 2440−2448.
(35) Samara, C.; Voutsa, D. Size distribution of airborne particulate matter and associated heavy metals in the roadside environment. *Chemosphere* **2005**, *59*, 1197−1206.
(36) Kujundzic, E.; Hernandez, M.; Miller, S. L. Particle size distributions and concentrations of airborne endotoxin using novel collection methods in homes during the winter and summer seasons. *Indoor Air* **2006**, *16*, 216−226.
(37) Traversi, D.; Alessandria, L.; Schiliro, T.; Gilli, G. Size-fractionated PM_{10} monitoring in relation to the contribution of endotoxins in different polluted areas. *Atmos. Environ.* **2011**, *45*, 3515−3521.
(38) Chung, M. Y.; Lazaro, R. A.; Lim, D.; Jackson, J.; Lyon, J.; Rendulic, D.; Hasson, A. S. Aerosol-borne quinones and reactive oxygen species generation by particulate matter extracts. *Environ. Sci. Technol.* **2006**, *40*, 4880−4886.
(39) Shen, G. F.; Wang, W.; Yang, Y. F.; Ding, J. N.; Xue, M. A.; Min, Y. J.; Zhu, C.; Shen, H. Z.; Li, W.; Wang, B.; Wang, R.; Wang, L.; Tao, S.; Russell, A. G. Emissions of PAHs from indoor crop residue burning in a typical rural stove: Emission factors, size distributions, and gas-particle partitioning. *Environ. Sci. Technol.* **2011**, *45*, 1206−1212.
(40) Choi, S. J.; Oh, J. M.; Choy, J. H. Toxicological effects of inorganic nanoparticles on human lung cancer A549 cells. *J. Inorg. Biochem.* **2009**, *103*, 463−471.
(41) Castillejos, M.; Borja-Aburto, V. H.; Dockery, D. W.; Gold, D. R.; Loomis, D. Airborne coarse particles and mortality. *Inhal. Toxicol.* **2000**, *12*, 61−72.
(42) McGuinnes, C.; Duffin, R.; Brown, S.; Mills, N. L.; Megson, I. L.; MacNee, W.; Johnston, S.; Lu, S. L.; Tran, L.; Li, R. F.; Wang, X.; Newby, D. E.; Donaldson, K. Surface derivatization state of polystyrene latex nanoparticles determines both their potency and their mechanism of causing human platelet aggregation in vitro. *Toxicol. Sci.* **2011**, *119*, 359−368.
(43) Asati, A.; Santra, S.; Kaittanis, C.; Perez, J. M. Surface-charge-dependent cell localization and cytotoxicity of cerium oxide nanoparticles. *ACS Nano* **2010**, *4*, 5321−5331.
(44) Bitterle, E.; Karg, E.; Schroeppel, A.; Kreyling, W. G.; Tippe, A.; Ferron, G. A.; Schmid, O.; Heyder, J.; Maier, K. L.; Hofer, T. Dose-controlled exposure of A549 epithelial cells at the air-liquid interface to airborne ultrafine carbonaceous particles. *Chemosphere* **2006**, *65*, 1784−1790.
(45) Knaapen, A. M.; Borm, P. J. A.; Albrecht, C.; Schins, R. P. F. Inhaled particles and lung cancer. Part A: Mechanisms. *Int. J. Cancer* **2004**, *109*, 799−809.